Tailored fibre placement of commingled carbon-thermoplastic fibres for notch-insensitive composites

El-Dessouky, H. M.; Saleh, M. N.; Gautam, M.; Han, G.; Scaife, R. J.; Potluri, P.

DOI
10.1016/j.compstruct.2019.02.043

Publication date
2019

Document Version
Final published version

Published in
Composite Structures

Composite Structures 214 (2019) 348–358

Contents lists available at ScienceDirect

Composite Structures

journal homepage: www.elsevier.com/locate/compstruct

Tailored fibre placement of commingled carbon-thermoplastic fibres for notch-insensitive composites

H.M. El-Dessouky[a,b,*,1], M.N. Saleh[c,*,1], M. Gautam[d], G. Han[e], R.J. Scaife[a], P. Potluri[d]

[a] Composite Centre, AMRC with Boeing, University of Sheffield, Rotherham S60 5TZ, UK
[b] Physics Department, Faculty of Science, Mansoura University, Mansoura 35516, Egypt
[c] Structural Integrity & Composites, Faculty of Aerospace Engineering, Delft University of Technology, Delft 2628 CD, The Netherlands
[d] School of Materials, University of Manchester, Oxford Road, Manchester M13 9PL, UK
[e] AMRC Korea, Gyeongsan, Gyeongsangbuk-do 38463, Republic of Korea

ARTICLE INFO

Keywords:
Thermoplastics
Tailored fibre placement
Composites
Mechanical properties
Notch sensitivity

ABSTRACT

Tailored fibre placement (TFP) is an embroidery-based technology that allows the fibre tows to be placed exactly where they are most needed for structural performance and stitched into position on a compatible textile or polymer substrate. In this study commingled carbon-nylon fibre tows were utilised to produce thermoplastic cross-ply net-shaped preforms using TFP. Four TFP composite plaques were manufactured; baseline (blank), machined-hole, tailored-hole-1 and tailored-hole-2. Steering the tows was used to create the hole in tailored-hole-1 and tailored-hole-2. In comparison to the design of tailored-hole-1, a different fibre trajectory, with a circular reinforcement around the hole, was suggested for the tailored-hole-2. Fibre volume fraction, optical microscopy, X-ray-CT scans, tensile and open-hole tests were carried out. With the exception of the baseline sample, the modified design of tailored-hole-2 composite exhibited the highest axial strength and modulus compared to the machined-hole and tailored-hole-1 composites. Only the tailored-hole-2 specimens exhibited less than 10% reduction of the notched strength compared to the un-notched strength. This study highlights the importance of the stress/load-paths and associated fibre-orientations. While TFP can be an extremely valuable design tool for composite preforms and resulting structural components, a deep understanding of stress distributions is inevitable to achieve optimal TFP-design.

1. Introduction

With an ever increasing demand for near net shape and lightweight parts for aerospace and automobile applications, carbon fibre-reinforced polymer (CFRP) composite materials have proven to be promising alternatives to their metal counterparts. This is due to their higher strength and stiffness to weight ratio, improved corrosion resistance and fatigue resistance. However, for many applications, CFRP composites requires joining with other metallic and composite parts, either mechanically or using adhesives. The mechanical joints such as rivets, pins and bolts can help in easy assembling and disassembling, when required for inspection, maintenance and repairing purposes without imparting damage [1–3]. The connections however, require introduction of holes and notches, which are generally drilled into the composites. Such machined-holes can introduce micro to macro scale defects leading to delamination and de-bonding between the reinforcement and matrix, which can significantly reduce the mechanical performance of the composite [4–9].

Although it is possible to reduce the extent of delamination, it cannot be eliminated completely. Several studies that have been conducted in this context, suggested using lower drill feed rate [10] which will help in reducing the thrust force exerted by the drill bit thereby reducing the extent of delamination, or using specialised drills instead of conventional twist drills, as the applied thrust force varies with the drill geometry and profile [5]. The use of double cone drills can help in reducing the thrust force [11], but cannot eliminate the delamination completely. Several other studies focussing on the reduction the delamination during drilling recommended usage of a back-up plate [12,13], but this technique has disadvantages. One being that high higher feed rates are required to drill the hole, which results in generation of higher thrust forces [14], and another that this strategy is useful when the opposite side of the plate is accessible, which often is not the case during repairs and maintenance.

Tailored fibre placement (TFP) technology offers a potential

* Corresponding authors.
E-mail addresses: h.el-dessouky@sheffield.ac.uk (H.M. El-Dessouky), m.a.s.n.saleh@tudelft.nl (M.N. Saleh).
[1] Contributed-equally.

https://doi.org/10.1016/j.compstruct.2019.02.043
Received 22 October 2018; Received in revised form 19 December 2018; Accepted 9 February 2019
Available online 11 February 2019

solution for manufacturing delamination-free holes. This technology, developed by Institute of Polymer Research Dresden [15], is an innovative technique in composite preforming that allows placement of the fibre tows along different trajectories (using CAD models), by locking their positions using simultaneous stitching. This method is based on the well-known embroidery technique to manufacture composite structures by arranging and laying the fibre where it is needed, and can be used for producing near-net shape preforms. The stitching action along the lateral direction in TFP process does not induce or have any significant effect on the strength of the material but it might affect its stiffness due to the waviness of the stitched tows [16].

The TFP produced thermoset composites with shaped hole have similar mechanical properties under cyclic tensile loading as non-crimped fabric (NCF) composites under cross-ply and angle-ply lay-up configurations [17]. They have proven that the open-hole laminates, with local fibre reinforcement, have similar strengths as the un-notched plates [18,19]. In addition, the TFP technology can be used to optimise the stress distribution along the weak sections of the composite (holes/notches) and reduce the non-preferred mode of failure [18,20].

Almost all studies reported in literature on TFP composites are based on thermoset polymer composites, there are limited or almost no studies reported with respect to thermoplastic TFP composites produced using commingled fibre tows. The objective of this paper is to study the mechanical properties of carbon/nylon 6 (CF/PA6) thermoplastic cross-ply composites, produced using TFP technology. Two different notched composites with tailored holes, each with different trajectory/fibre path around the hole, are designed, manufactured and tested under tension. The produced laminates are also physically characterised by fibre volume fraction analysis and optical microscopy. In addition their tensile behaviour is studied and compared with machined/drilled hole and baseline “un-notched” composites also produced using TFP technology.

2. Materials and manufacturing

The Carbon fibre, used in this study, is Grafil 34-700 continuous, PAN based fibre, 12 k of linear density 800 tex and high strength [21]. The thermoplastic matrix (fibre), backing material (film) and stitching thread (fine yarn) are all made of the same polymer, Nylon-6 (PA6).

2.1. Commingled tow characterisation

The optical micrographs of the cross-section of the commingled tow (Fig. 1) were not taken by setting the commingled tows in a resin pot, as this process may lead to dispersion of the filaments (both reinforcement and thermoplastic) from their original location, thereby leading to changes in fibre distribution, instead the micrographs were obtained from careful slicing of the dry fibre tow to obtain as accurate results as possible.

The fibre distribution of the components in the commingled tow, in terms of radial distribution index and lateral distribution index were computed using Eq. (2.1) and Eq. (2.7) respectively. The process of calculating the radial distribution & lateral distribution index, and blend quality coefficient are reported in this section. The Eqs. (2.1) to (2.9) are based on the studies conducted in [22,23].

In order to calculate radial distribution index (R_d) of the tow containing the commingled filaments using Eq. (2.1), the radius of the cross-section formed by the reinforced filaments (R_{re}) and the thermoplastic filaments (R_{tf}) is required, which is calculated using Eqs. (2.2) & (2.3).

$$R_d = \frac{R_{re}}{R_{tf}} \tag{2.1}$$

$$R_{re} = \frac{\sum_{i=1}^{N_{re}} \sqrt{[X_{re}(i) - C_x]^2 + [Y_{re}(i) - C_y]^2}}{N_{re}} \tag{2.2}$$

$$R_{tf} = \frac{\sum_{i=1}^{N_{tf}} \sqrt{[X_{tf}(i) - C_x]^2 + [Y_{tf}(i) - C_y]^2}}{N_{tf}} \tag{2.3}$$

To calculate the values of R_{re} and R_{tf}, the centre coordinates of the cross-section formed by each reinforcement (C_{xre}, C_{yre}) and thermoplastic (C_{xtf}, C_{ytf}) component are first calculated using Eqs. (2.4) and (2.5), respectively. The coordinates obtained for each component are then averaged out to obtain the average centre coordinate of the commingled tow cross-section using Eq. (2.6). In Eqs. (2.4) & (2.5), N_{re} and N_{tf} refer to the total number of reinforced filaments and thermoplastic filaments respectively, and X_{re}, Y_{re} refer to the x,y coordinates of each reinforced filament at (i) number (similarly for X_{tf}, Y_{tf}).

$$C_{xre} = \frac{\sum_{i=1}^{N_{re}} X_{re}(i)}{N_{re}}, \quad C_{yre} = \frac{\sum_{i=1}^{N_{re}} Y_{re}(i)}{N_{re}} \tag{2.4}$$

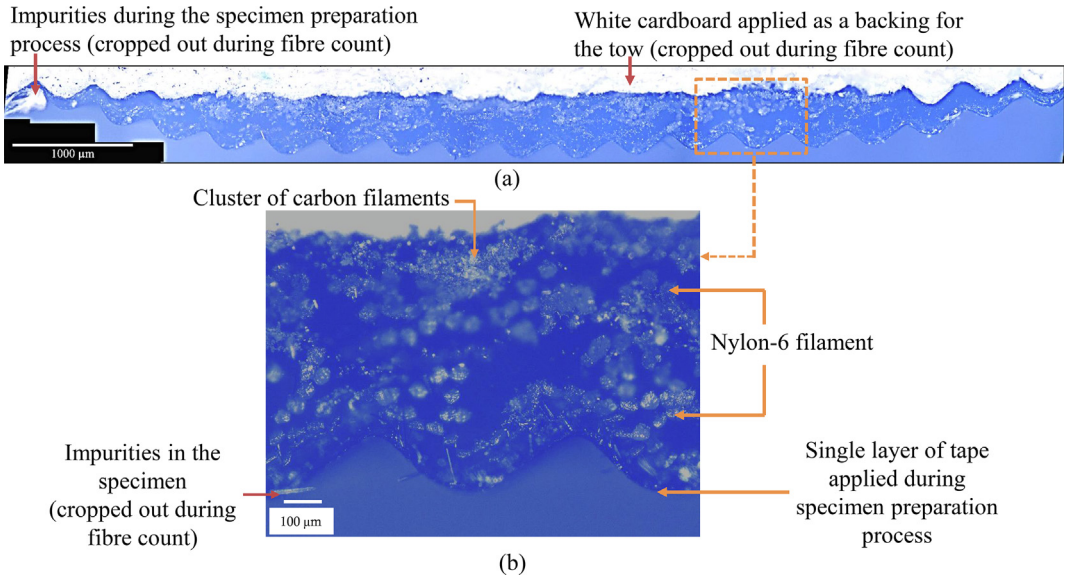

Fig. 1. Optical micrograph of (a) whole and (b) segment of carbon and nylon-6 commingled tow.

$$C_{xtf} = \frac{\sum_{i=1}^{N_{tf}} X_{tf}(i)}{N_{tf}}, \quad C_{ytf} = \frac{\sum_{i=1}^{N_{tf}} Y_{tf}(i)}{N_{tf}} \tag{2.5}$$

$$C_x = \frac{C_{xre} + C_{xtf}}{2}, \quad C_y = \frac{C_{yre} + C_{ytf}}{2} \tag{2.6}$$

The lateral distribution index (L_t) is calculated using Eq. (2.7), with the centre coordinates of reinforcement filaments (C_{xre}, C_{yre}), the average centre coordinates of all the whole tow (C_x, C_y), and R_a (calculated using Eq. (2.8)).

$$L_t = \frac{\sqrt{(C_{xre} - C_x)^2 + (C_{yre} - C_y)}}{R_a} \tag{2.7}$$

$$R_a = \frac{\sum_{i=1}^{N_{re}} \sqrt{[X_{re}(i) - C_x]^2 + [Y_{re}(i) - C_y]^2}}{N_{tf} + N_{re}} + \frac{\sum_{i=1}^{N_{tf}} \sqrt{[X_{tf}(i) - C_x]^2 + [Y_{tf}(i) - C_y]^2}}{N_{tf} + N_{re}} \tag{2.8}$$

The blend quality coefficient (K_b) is calculated using Eq. (2.9), using radius of the cross-section formed by the reinforcement filaments (R_{re}) and the lateral distribution index (L_t) of the commingled tow. The blending quality coefficient found for Carbon & Nylon 6 filaments was found to be 0.000043 ± 0.000026, which can be considered to be close to perfect blend ($K_b = 0$, is perfect blend).

$$K_b = |1 - R_{re}|. L_t \tag{2.9}$$

This value has been compared with studies conducted in [22,24], where the blend quality coefficient has been reported between 0.15 and 0.40, for Glass and Propylene commingled tow in [22]. In the other study conducted in [article] on the commingled Glass and Polyamide tow, K_b value of 0.21 was reported. Both these studies [22,24], examined a cross-section with less than 1000 filaments, which help in inferring the blend quality of Carbon & Nylon 6, commingled tow (with ~12200 filaments) to be close to perfect.

2.2. Preform design and composite manufacturing

For specimens' production, three different designs were implemented to produce the required types under investigation in this study as depicted in Fig. 2.

The common for all of the preforms was the layup being a symmetric cross-ply laminate layup $[0_2/90/0]_S$ with only two plies at the 90° direction. Such layup was suggested just to proof the concept and to demonstrate the potential of technology and not to simulate a real layup for bolted joints in practice. Fig. 3 demonstrates the whole manufacturing process starting with the TFP of the commingled preform at an instance in which a 0° layer is completed while the 90° layer is being placed (see Fig. 3a). The other common aspect was the consolidation profile for all the preforms (see Fig. 3b) to produce the composite specimens of nominal thickness ~3 mm. The tool plus the preforms were heated up under pressure (~1 bar) in the press at 270 °C for 15 min. Then they were cooled down outside the press at room temperature for 10 min. Fig. 3c shows the consolidated specimens before extracting them from the tool.

The first TFP design was used for both the baseline/notch free specimens as well as the specimens drilled afterwards to produce the machined-hole specimens. In this design, minimal steering of the commingled tows was required in the middle of the specimen's length as there was no need to create the hole (see Fig. 4). Holes were drilled using a two-fluted, 6 mm diameter, High Strength Steel (HSS) drill bit with a 90° point angle. Conservative cutting speed of approximately 100 mm/min and feed of 0.05 mm/rev were used to ensure acceptable hole quality was achieved. The second TFP design was implemented to produce the first type of the TFP-hole specimens in which the commingled tow steering varies from one layer to the other. As depicted in Fig. 4, the outer most layer was a 0° orientation with the commingled tow steered as a semi-circular reinforcement around the hole from the left (L) hand side. While the layer below repeated the same steering pattern but the reinforcement was from the right (R) hand side. Due to steering the commingled tow around the hole in one single direction, this created a gap on the top and the bottom halves of the preform which had to be compensated with looping back the following tow in a U-shape towards the edge of the perform/specimen as highlighted in Fig. 4 (tailored-hole-1). This loop-back effect on the mechanical properties and performance of the consolidated specimens is discussed in Section 4.2. For the remaining 0° and 90° plies, the central (C) steering was used in which two commingled tows are driven symmetrically around the hole. This did not create any gaps in the TFP process unlike the L and the R steering in the first TFP hole design. Thus, no compensation was needed.

The third and final TFP design (tailored-hole-2) was mainly implemented to overcome the loop-back issue highlighted previously in the first TFP design. Besides, it represents a good comparison case to highlight the effect of the TFP design 'tow steering' on the mechanical performance/properties of notch-created preforms/composites. The main advantage of this design is that all the layers were of the central steering type (C). Thus, no gaps or loop-back tows existed in this design. To further enhance the hole periphery, a circular reinforcement was created by steering one commingled tow around the hole in the design as shown in Fig. 4 (tailored-hole-2).

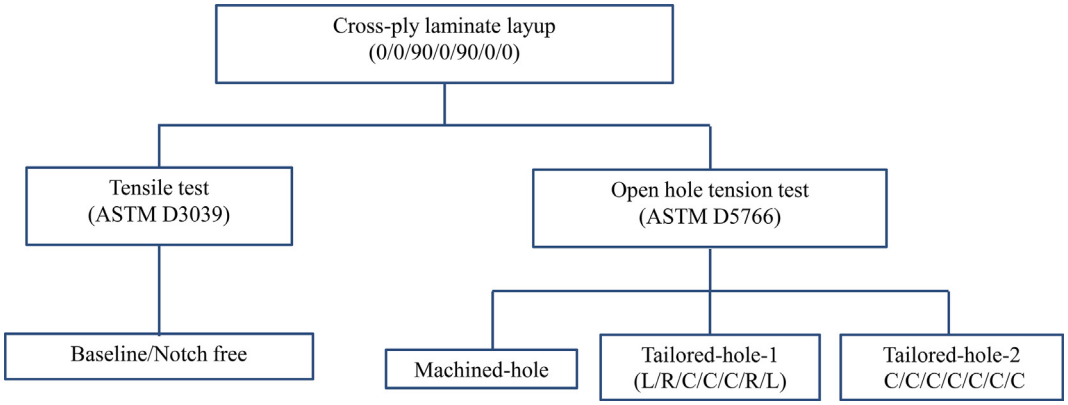

Fig. 2. Schematics of TFP layup of composite samples investigated in this study, C refers to the two central tows steered symmetrically around the hole, L & R are the steered tows from the left and right hand sides of the hole.

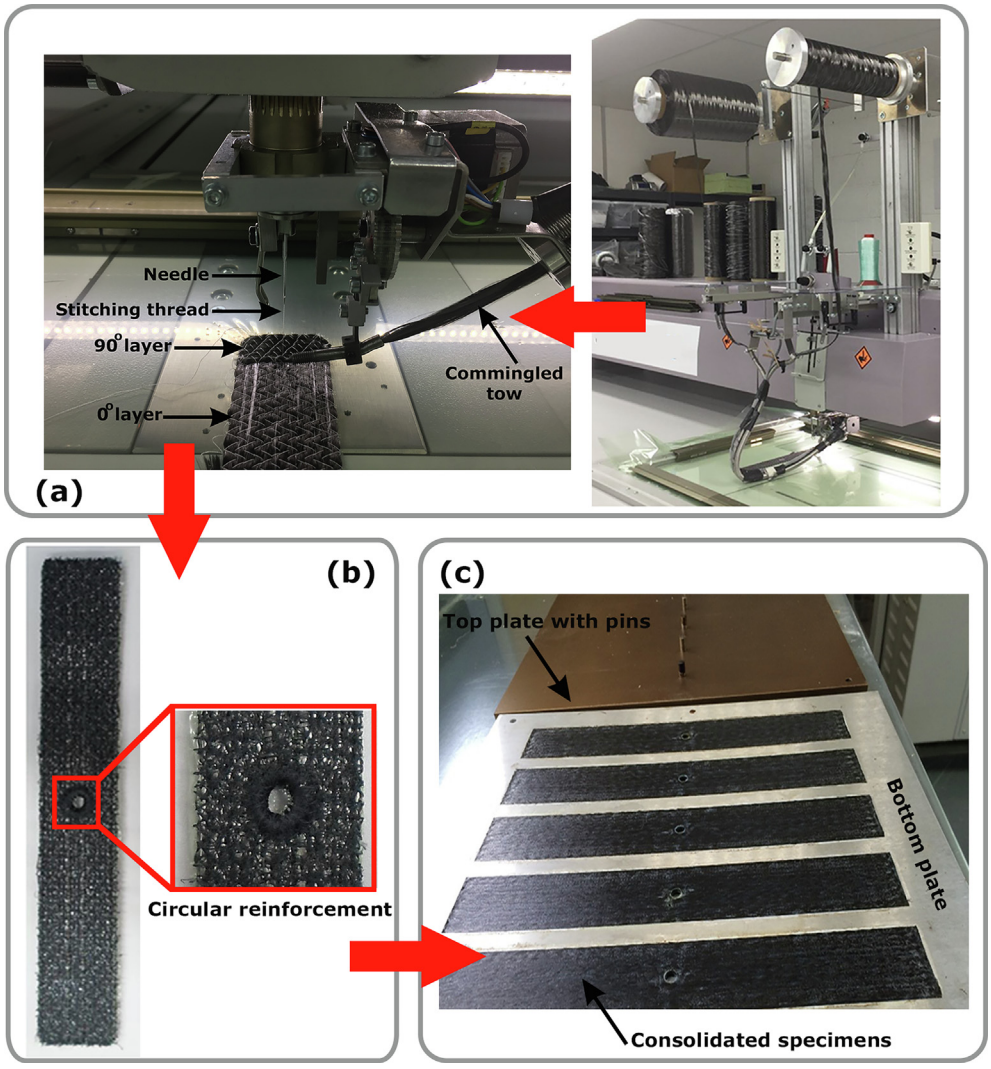

Fig. 3. Manufacturing process: (a) TFP process of the commingled preform at an instance in which a 0° layer is completed while the 90° layer is being placed, (b) one example of a preform showing the circular reinforcement around the hole and (c) consolidated specimens before extraction from the tool.

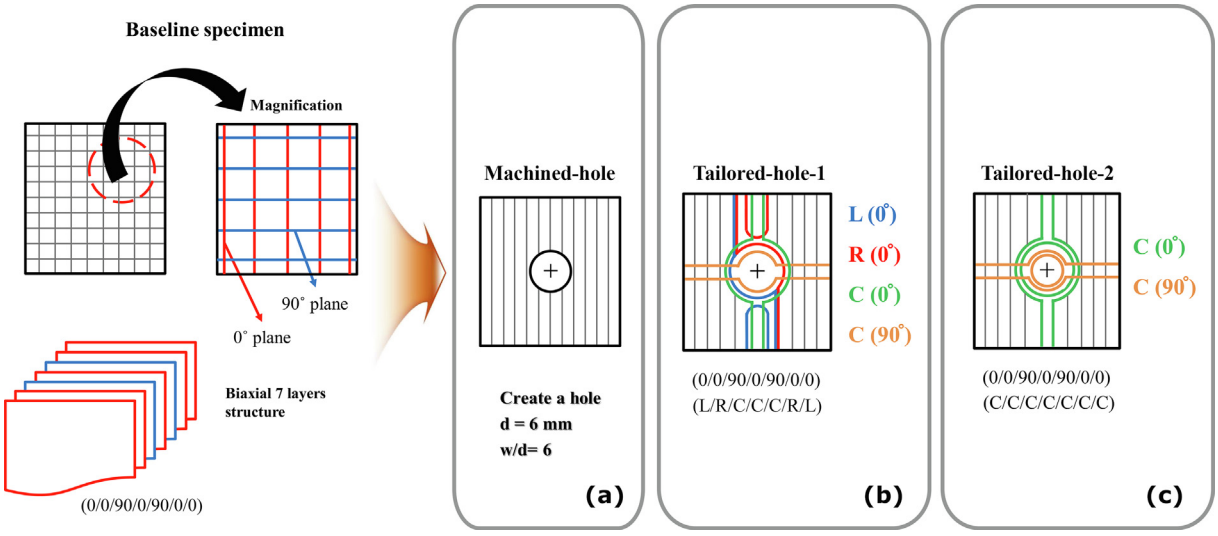

Fig. 4. Schematic showing the layup and trajectory of fibre tow placement for the different types of TFP specimens.

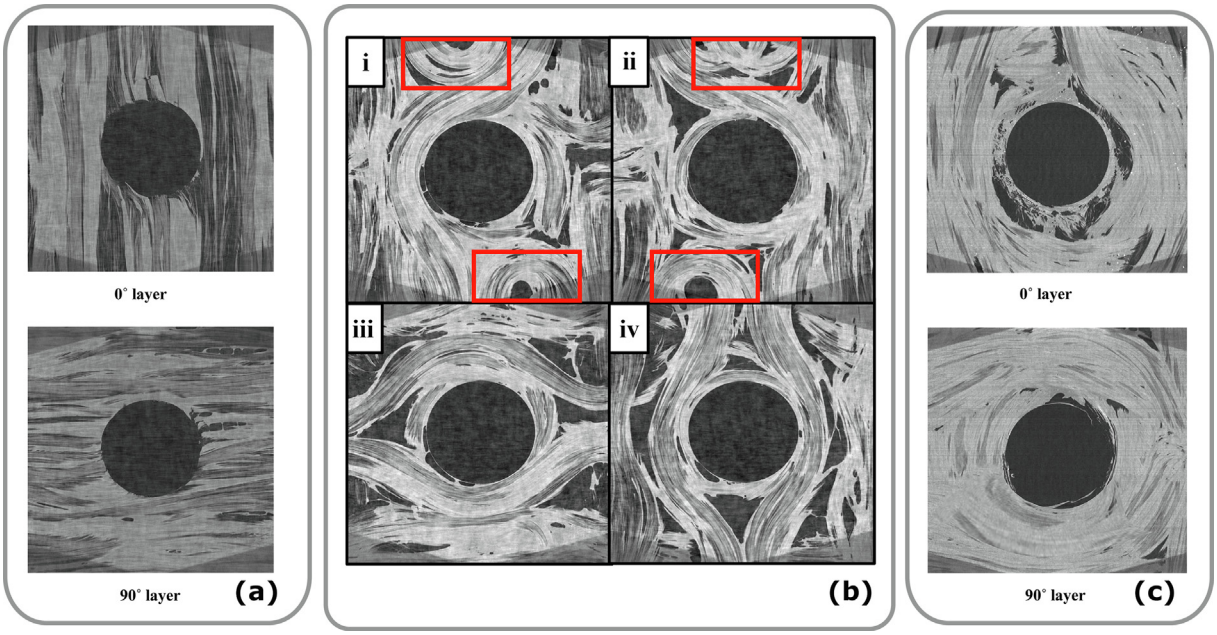

Fig. 5. X-ray CT scans of carbon/nylon-6 composite specimens with (a) Machined-hole, (b) Tailored-hole-1 and (c) Tailored-hole-2.

3. Experiment and characterisation

3.1. Physical characterisation

3.1.1. X-ray computed tomography (CT)

To examine the as manufactured composite specimens, X-ray CT scans were performed for the three different types of notched specimens using a Zeiss Xradia Versa XRM-520. The 0.4x objective of the scanner was used. The total volume in the field of view was 16 × 16 × 16 mm^3, resulting in a voxel size of ~7.8 µm. The source voltage and current were set to 40 kV and 75 µA respectively. The exposure time for each radiograph was 20 s, with 1017 radiographs being collected over 360°. The total data acquisition time was 6 h. After scanning, the 3D volume was reconstructed out of the 2D X-ray radiographs and cross-sectional slices were captured to highlight the commingled tow's path (see Fig. 5).

As expected from the X-ray CT cross-sectional images, the drilling process resulted in broken fibres in the case of machined-hole which would have an effect on the mechanical behaviour as discussed in Section 4.2. In addition, the four different layers of the first TFP design for the hole (0°-L, 0°-R, 90°-C and 0°-C) are clearly identified from the X-ray slices as (i), (ii), (iii) and (iv) respectively in Fig. 5b. The path of the steered commingled tows is clearly recognised as well as the loop-back tows highlighted by the red rectangles in Fig. 5b. It is also clear that the loop-back tows are not centred in Fig. 5b. There could be two possible reasons for this misalignment. The first is that the path of the loop-back tow is affected by the closest tow, which is either the left or the right steered tow. The second reason could be distortions due to the consolidation process during applying the pressure by the tool. The applied heat causes the stitching thread to melt as well as the thermoplastic component of the tow. Thus, the location of the tows might slightly deviate during consolidation. Moreover, resin rich regions around the hole exist in a significant manner compared to the machined/drilled holes. For the tailored-hole-2 design, the resin rich regions and the voids around the whole are drastically reduced by adding the extra circular reinforcement tow in each layer. The path of the central tows in the 0° layer clearly goes from the top edge and has a curvature to accommodate the hole in the middle. Similarly in the 90° layer, the same pattern is observed but the difference is that this time the path goes from one side of the specimen to the other which is from right to left in this case (see Fig. 5c).

3.1.2. Fibre volume fraction analysis

In order to examine the quality and integrity of composite specimens manufactured in this study, fibre volume fraction (V_f) tests were conducted in accordance with ASTM D3171 standard [25] using the matrix burn-off test "Procedure G". The specimens were pre-conditioned as per ASTM D5229 [26]. Five specimens were tested for each TFP composite configuration; the length of the specimens was 10 mm and the width was kept same as the sample's width. The density of the specimens was determined before the burn-off using Mettler Toledo density meter. Afterwards, the laboratory chamber furnace, from Carbolite, was adjusted at 550 °C for the burn-off. The duration of the burn-off for each specimen was ~25 min.

3.2. Mechanical testing

The test set up and the specimen dimensions have been shown in Fig. 6. The length of all specimens were kept the same however, the width of baseline specimen was kept consistent at ~25 mm and for notched specimen consistent width of ~36 mm was used for all specimens. Glass & Epoxy fabric composite tab with 50 mm length was applied on both ends and both sides of the carbon/nylon-6 composite specimen (as shown in Fig. 6b). The baseline specimens were tested conforming to ASTM D3039 [27], whilst the notched specimen with a hole diameter of 6 mm were tested according to ASTM D5766 [28]. Five specimens were tested for the baseline specimens while six specimens were tested for the machined and each type of the TFP open-hole specimens. The test was carried out on an Instron 5982 test machine, with servo-hydraulic grips with a load cell capacity of 100 kN and the axial strains were recorded using Imetrum Video Extensometer (test setup shown in Fig. 6a).

4. Results and discussion

4.1. Fibre volume fraction

The V_f values and their standard deviations for all types of TFP composites investigated are shown in Table 1. The V_f values for all were found to be similar with maximum deviation of 1.02% between

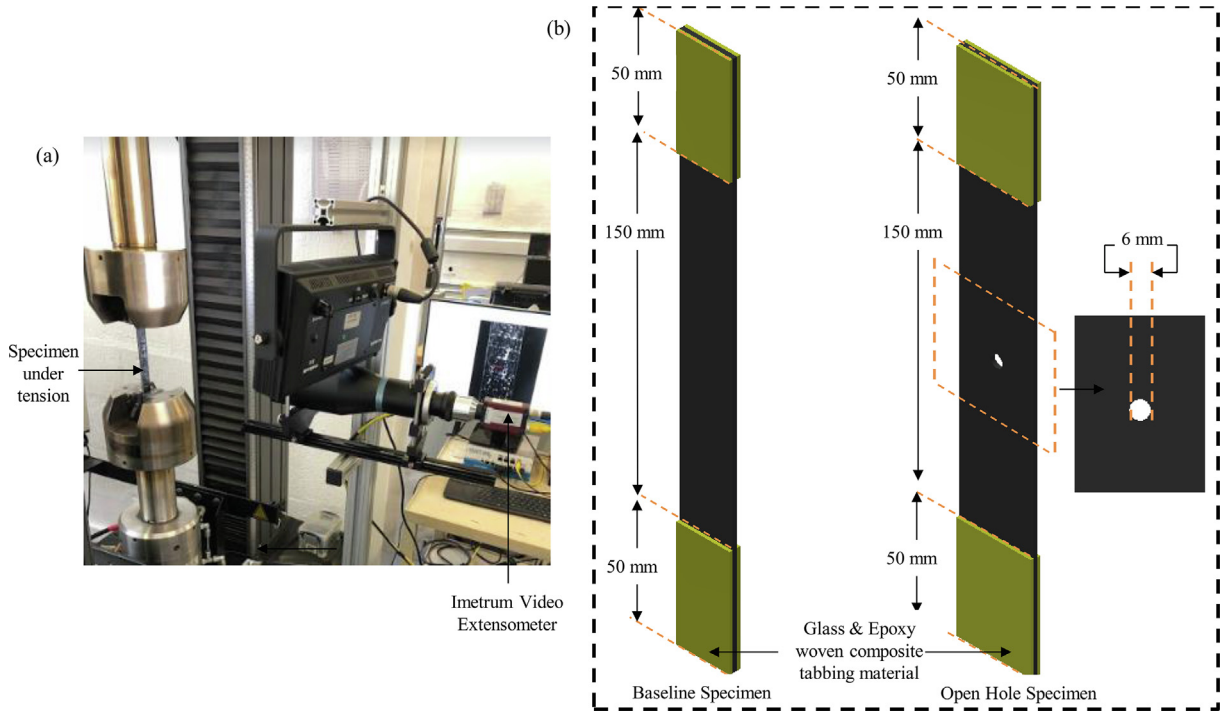

Fig. 6. (a) Test set-up for open hole tension test, and (b) schematics of test specimens.

Table 1
Density & fibre volume content for the different types of TFP composite specimens.

Type	Density (%)	Fibre volume content (%)
Baseline	1.09 ± 0.01	35.10 ± 0.05
Machined-hole	1.10 ± 0.01	34.18 ± 0.43
Tailored-hole-1	1.05 ± 0.02	33.65 ± 1.99
Tailored-hole-2	1.13 ± 0.01	34.51 ± 0.55

tailored-hole-1 and the baseline specimens. The similar V_f values between different TFP types of specimens investigated help in better comparison of their mechanical properties.

To estimate the voids content in all the manufactured specimens, optical microscopy was used and optical cross-sectional images were analysed at different locations of the specimens. A selection of a total of 80 processed images is depicted in Fig. 7. Images were processed based on the grey scale using the ImageJ software assuming the bright 'white' represents the carbon fibres, grey represents the matrix and the dark 'black' represents voids. Statistical analysis was carried out and it was concluded that the average voids content (%) in all specimens, regardless of their type, around 9.10 ± 3.55. This relatively higher voids content compared to thermoset composites [29] can be attributed to the quality of the commingled thermoplastic/CFRP tows which still represents a challenge for such technology, but also a room for future improvement.

4.2. Mechanical testing

4.2.1. Stress-strain response

The global stress-strain curves for the baseline, open-hole machined, open-hole TFP 1 and open-hole TFP 2 specimens are depicted in Fig. 8a-d respectively. As highlighted previously, five specimens were tested for the baseline while six specimens were tested for all types of open-hole specimens. The stress-strain curves demonstrate good repeatability of all the tested specimens. As expected from the laminate lay-up, baseline specimens demonstrate brittle behaviour with a linear response up to failure (see Fig. 8a). Similar behaviour is observed for both open-hole TFP specimens with a shorter damage progression stage just before final failure (see Fig. 8c & d). On the contrary, the machined open-hole specimens clearly demonstrate the damage progression effect on the initial stiffness by a reduction in the slope of the stress-strain curve. Starting from approximately 0.8% strain, the stiffness of the machined open-hole specimens reduces significantly up till failure. The second linear curve is associated with matrix cracking and inter-yarn matrix delamination that leads to gradual change of stiffness before the final fracture due to fibre breakage. Table 2 summarises the tensile modulus, tensile strength and failure strain data for all the specimens tested. It is clear from the summary that the baseline specimens demonstrate the stiffest response (~37 GPa) and the highest tensile strength (~429 MPa) with the least strain-to-failure value (~0.95%). The effect of notch creation is then captured by the effect it has on the tensile modulus and strength of the three notched composites: machined-hole, tailored-hole-1 and tailored-hole-2.

Creating notches/holes in CFRP laminates with machining/drilling has been extensively studied in the literature and as reported in the introduction, it significantly reduces the tensile modulus and strength of the laminates due to the damage induced during the machining process [4–9]. Thus, it would have made a reasonable sense if the machined-hole specimens had the least tensile modulus and strength compared to the tailored-hole specimens. However, experimental results indicate that the machined-hole specimens are stiffer (~26 GPa) than one of the TFP-created-hole specimens (~20 GPa) which is tailored-hole-1 specimens, with almost no difference in the tensile strength. This can be attributed to the design process of this type of TFP-created-hole specimen as previously observed and reported in [19]. The inferior behaviour of this design is mainly due to the fact that the tow path is not continuous from on edge of the specimen to the other along the length direction. In order to create the hole mainly in the 0° plies, the tow had to be driven around the hole and the next longitudinal tow had to loop back to the edge to fill in the gap that was created by steering the one before as highlighted previously in Section 2.2 in Fig. 4 (tailored-hole-1).

This loop-back effect is more profound in the tensile modulus

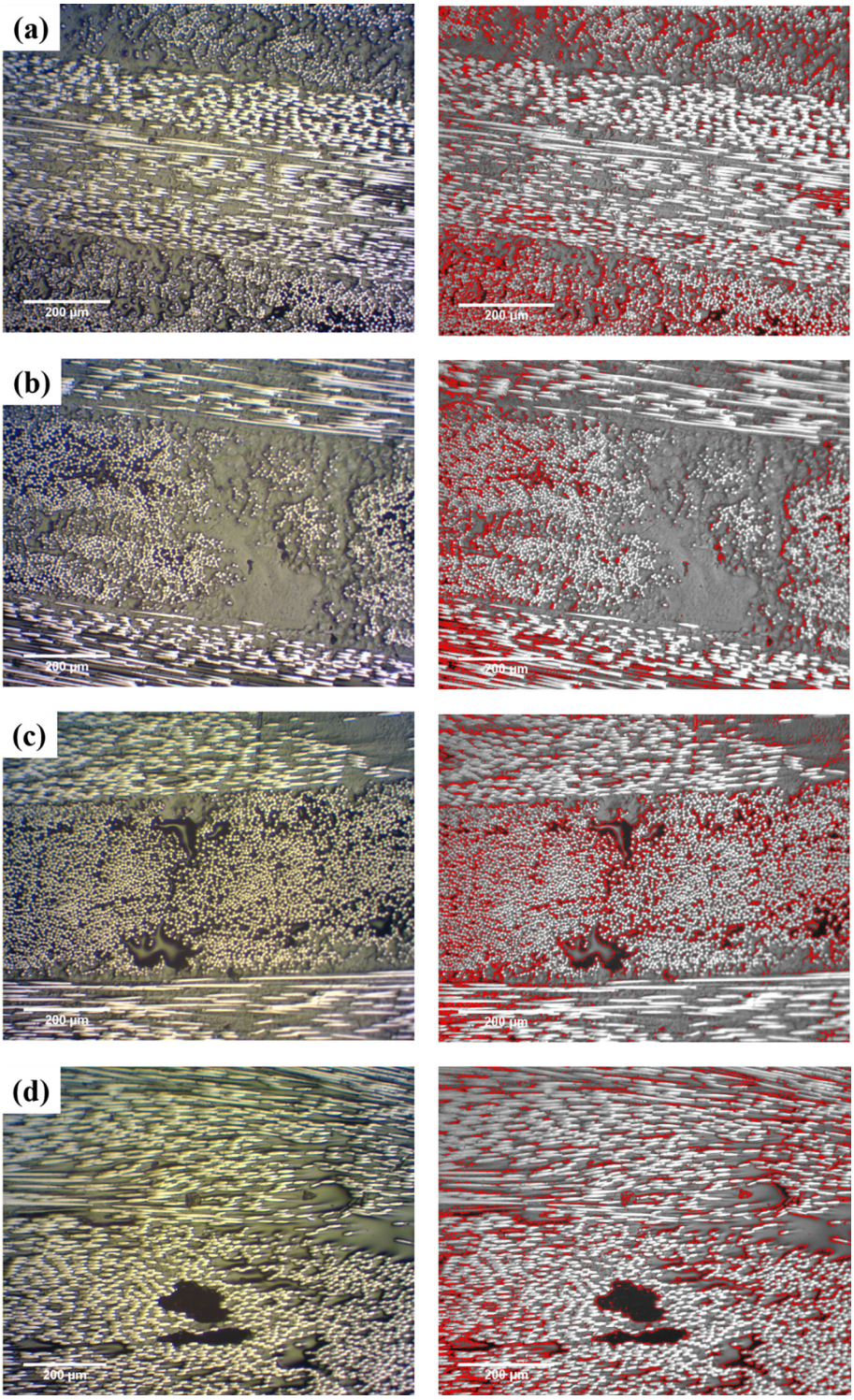

Fig. 7. A selection of optical cross-sections of the TFP specimens: original micrographs (left) and their processed images (right).

compared to the tensile strength. This highlights the need of proper understanding of the stress/load-paths and associated fibre-orientations. While TFP can be an extremely valuable design tool for composites and resulting structural components, a deep understanding of stress distributions is inevitable, to obtain optimal TFP-design. Consequently, tailored-hole-2 type of specimens was designed to avoid this fibre interruption phenomena and still provide reinforcement around the notch. From experimental results (see Fig. 9a–c), the solution proves to be effective as the tailored-hole-2 specimens demonstrate the least reduction in tensile modulus (~33 GPa) and tensile strength (~392 MPa) among the other notched specimens and compared to the baseline one. Similar trend has been reported for thermoset composites in [18,19]. This comparison between all types for notch sensitivity analysis is discussed in the following section.

As previously reported by Saleh et al. [30], there are two approaches when it comes to design of composite materials based on the target application. These two approaches are the strength-design based approach and the energy/toughness-based approach. For this purpose,

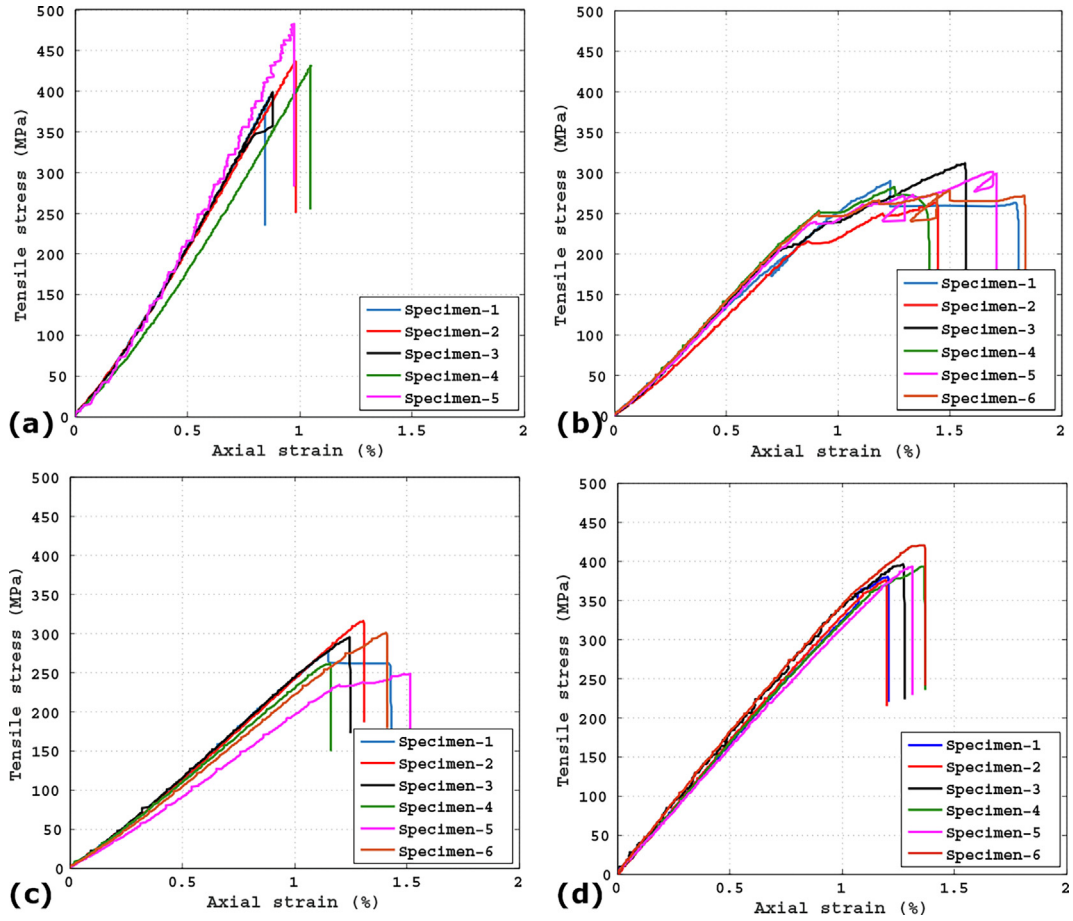

Fig. 8. Stress-strain curves for: (a) Baseline, (b) Machined-hole, (c) Tailored-hole-1 and (d) Tailored-hole-2 specimens.

Table 2
Summary of the mechanical properties of the tested specimens.

Type	Tensile modulus (GPa)	Tensile strength (MPa)	Failure strain (%)
Baseline	36.74 ± 2.68	429.00 ± 32.54	0.95 ± 0.07
Machined-hole	25.65 ± 1.39	287.83 ± 15.81	1.44 ± 0.16
Tailored-hole-1	20.10 ± 1.78	285.50 ± 21.51	1.29 ± 0.13
Tailored-hole-2	33.25 ± 2.23	392.28 ± 14.59	1.28 ± 0.07

the energy absorption per unit volume up to fracture (in MJ/m^3) is calculated as the area under the stress-strain curve for all the tested samples. Fig. 9d summarises the comparison for all the types. It is clear that the tailored-hole-2 type has higher energy absorption (~2.75 MJ/m^3) compared to both the baseline (~1.78 MJ/m^3) and tailored-hole-1 (~1.99 MJ/m^3) specimens, while the machined-hole specimens demonstrate more energy absorption capability (~2.98 MJ/m^3). This definitely comes over the cost of sacrificing the stiffness and strength of the materials as highlighted earlier in this section. Thus, the only type of specimens that relatively keeps the balance and trade-off between high strength and high energy absorption is the innovative design of the tailored-hole-2.

4.2.2. Notch sensitivity analysis

For an isotropic material, the Stress Concentration Factor (SCF) of a hole in an infinite plate [31] is approximately 3. Composites are not isotropic in nature; actually they are anisotropic material systems in which the material response is completely dependent on the lay-up. For orthotropic laminates loaded at an angle from their principal directions [32], the SCF varies between (0 and 8) times the global stress applied. In order to evaluate the notch sensitivity of the tested machined and TFP specimens 'at this specific hole diameter to width ratio', the notched tensile strength is normalised by the un-notched strength. Then, the normalised value is compared against the ideally ductile "notch insensitive" curve and the ideally brittle "notch sensitive" curve as shown in Fig. 10.

Equations for the notch sensitive and notch insensitive responses [33] are detailed as follows:

In the case of notch insensitive (ductile materials)

$$\sigma_n/\sigma_{un} = 1 - (D/W) \tag{4.1}$$

where:

σ_n: The notched tensile strength
σ_{un}: The un-notched tensile strength
D: The hole diameter
W: The specimen width

In the case of notch sensitive (brittle materials),

$$\sigma_n/\sigma_{un} = [1 - (D/W)]/K_T \tag{4.2}$$

where

$$K_T = 2 + [1 - (D/W)]^3 \tag{4.3}$$

It is clear from the comparison that there is a significant difference in the notch sensitivity between the three types of tested specimens. Both the machined-hole and tailored-hole-1 specimens experienced a drastic reduction of strength due to the notch creation. Approximately 35% of the tensile strength is sacrificed by the hole introduction. On the contrary, the tailored-hole-2 specimens demonstrate relatively a notch insensitive response 'at this specific hole diameter to width ratio'. The

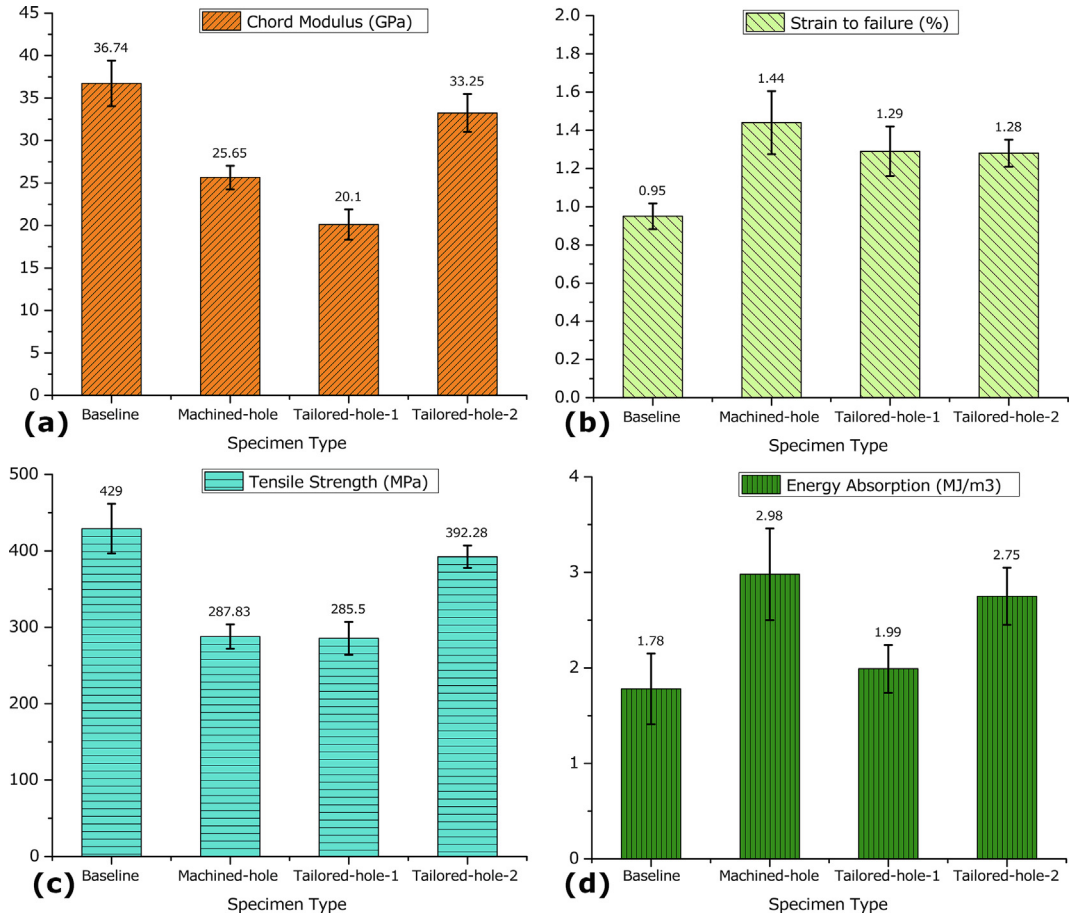

Fig. 9. Summary of test results: (a) Chord Modulus, (b) Strain to Failure (%), (c) Tensile Strength (MPa) and (d) Energy Absorption (MJ/m^3).

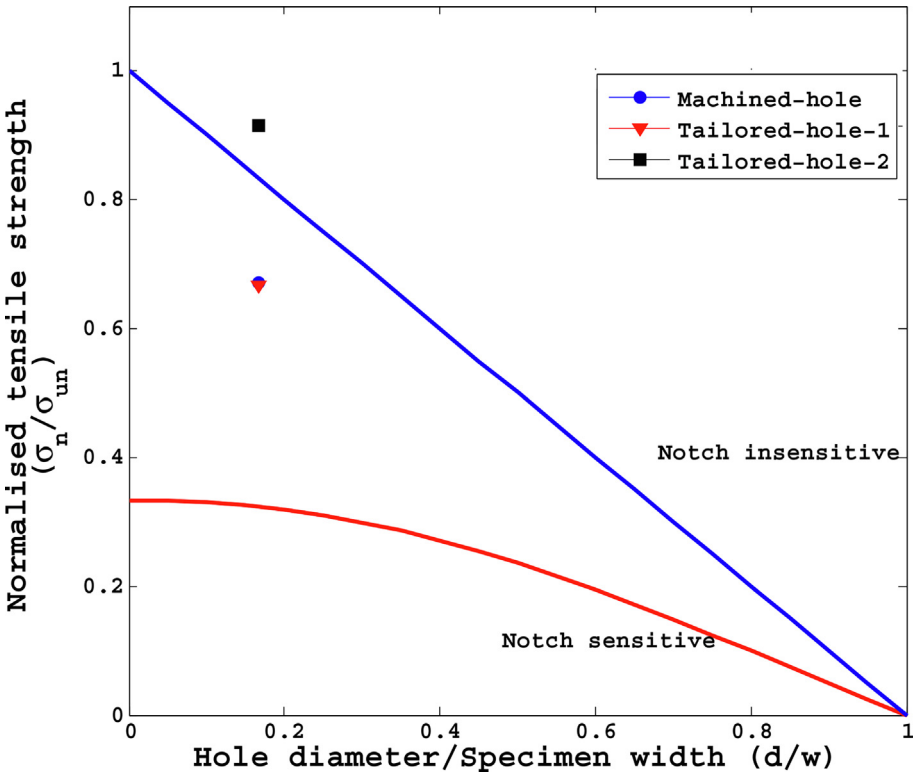

Fig. 10. Notch sensitivity study for Machined-hole, Tailored-hole-1 and Tailored-hole-2 specimens.

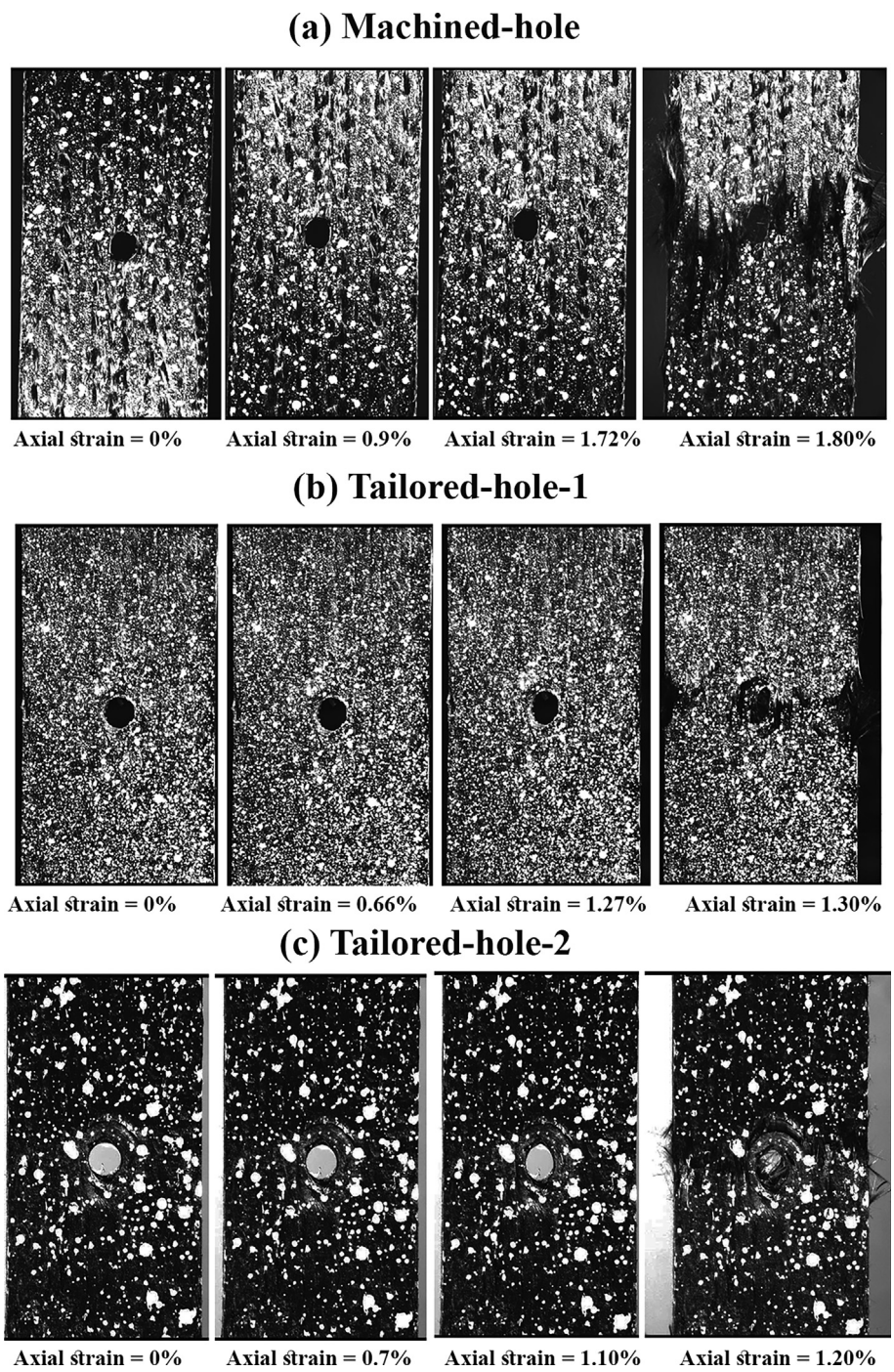

Fig. 11. Images of specimen under tension at different strain levels for (a) Machined-hole, (b) Tailored-hole-1 and (c) Tailored-hole-2 specimens.

tensile strength reduction for this type of specimens is less than 10%. The apparent difference in notch sensitivity can be explained/interpreted in the light of the specimen design and hole-creation process. From the design point of view, the tailored-hole-2 specimens have an extra circular tow reinforcement around the hole with no fibre interruption or cuts along the specimen length unlike the tailored-hole-1 specimens where fibres do not run continuously from one edge of the specimen to the other edge, however they loop back instead. This helps in reducing the size of the resin rich region introduced around the notch/hole which represents a critical/weak point in the design of tailored-hole-1 specimens. From the hole-creation process point of view, no delamination or matrix cracking is introduced due to the notch creation such as the ones experienced in the machined-hole specimens [4–9]. This all leads to the relatively superior notch-insensitive behaviour of the tailored-hole-2 compared to the tailored-hole-1 and the machined-hole specimens.

The deformation/damage of the three notched specimens: machined-hole, tailored-hole-1 and tailored-hole-2 is shown at different strain levels in Fig. 11, where visually the machined specimens do not show that much deformation of the hole before the final failure. However, the tailored-hole-1 specimens show some deformation from circular to elliptical shape and the largest deformation is clear in the tailored-hole-2 specimens. In addition, the machined specimen demonstrate catastrophic failure with extensive fibres breakage that spans the full width of the specimen. For tailored-hole-1 specimen, the hole deformation at failure is accompanied with fibre breakage. The failure

is a bit more contained in the tailored-hole-2 design as the circular reinforcing tow around the hole plays a role in the final failure.

5. Conclusion

TFP technology has been proven as a promising technique and has the potential to replace the conventional machining process for machining of hole-structured composites using commingled (CF/PA6) tows. The notched response of three different types of specimens; machined-hole, tailored-hole-1 and tailored-hole-2 was compared to the baseline/un-notched response. Based on the results obtained and discussed in this study, the following remarks are concluded:

- Fibre can be placed where the reinforcement is needed using TFP.
- All the notched samples experienced lower stiffness and strength compared to the baseline.
- The tailored-hole-2, with less fibre interruption, no looping and circular fibre around the hole, demonstrated the least reduction in mechanical properties, with a tensile modulus of (~33 GPa) and tensile strength of (~392 MPa), among the other notched specimens.
- The innovative tailored-hole-2 exhibited a relatively superior notch-insensitive behaviour (less than 10% reduction in tensile strength) compared to the tailored-hole-1 and the machined-hole specimens.

In summary, this study highlights the importance of proper understanding of the stress/load-paths and associated fibre-orientations. Although TFP can be an extremely valuable design tool for composites and resulting structural components, a deep understanding of stress distributions is inevitable, to obtain optimal TFP-design.

Acknowledgments

Authors would like to acknowledge Shape Machining Ltd and Coats for supporting this research.

Appendix A. Supplementary data

Supplementary data to this article can be found online at https://doi.org/10.1016/j.compstruct.2019.02.043.

References

[1] Atas A, Mohamed GF, Soutis C. Modelling delamination onset and growth in pin loaded composite laminates. Compos Sci Technol 2012;72:1096–101. https://doi.org/10.1016/j.compscitech.2011.07.005.
[2] Ataş A, Mohamed GF, Soutis C. Progressive failure analysis of bolted joints in composite laminates. Plast Rubber Compos 2012;41:209–14. https://doi.org/10.1179/1743289811Y.0000000038.
[3] Ataş A, Soutis C. Strength prediction of bolted joints in CFRP composite laminates using cohesive zone elements. Compos Part B Eng 2014;58:25–34. https://doi.org/10.1016/j.compositesb.2013.10.017.
[4] Capello E, Tagliaferri V. Drilling damage of gfrp and residual mechanical behavior – Part I: drilling damage generation. J Compos Technol Res 2001;23:122–30.
[5] Hocheng H, Tsao CC. Effects of special drill bits on drilling-induced delamination of composite materials. Int J Mach Tools Manuf 2006;46:1403–16. https://doi.org/10.1016/j.ijmachtools.2005.10.004.
[6] Kwon YW, Lee JH, Liu CT. Study of damage and crack in particulate composites. Compos Part B Eng 1998;29:443–50. https://doi.org/10.1016/S1359-8368(98)80002-4.
[7] Kwon YW, Berner JM. Micromechanics model for damage and failure analyses of laminated fibrous composites. Eng Fract Mech 1995;52:231–42.
[8] Saleh MN, Soutis C. Recent advancements in mechanical characterisation of 3D woven composites. Mech Adv Mater Mod Process 2017;3. https://doi.org/10.1186/s40759-017-0027-z.
[9] Saleh MN, Wang Y, Yudhanto A, Joesbury A, Potluri P, Lubineau G, et al. Investigating the potential of using off-axis 3D woven composites in composite joints' applications. Appl Compos Mater 2016;24:377–96. https://doi.org/10.1007/s10443-016-9529-9.
[10] Davim JP, Reis P. Drilling carbon fiber reinforced plastics manufactured by autoclave-experimental and statistical study. Mater Des 2003;24:315–24. https://doi.org/10.1016/S0261-3069(03)00062-1.
[11] Zitoune R, El Mansori M, Krishnaraj V. Tribo-functional design of double cone drill implications in tool wear during drilling of copper mesh/CFRP/woven ply. Wear 2013;302:1560–7. https://doi.org/10.1016/j.wear.2013.01.046.
[12] Ataş A, Gautam M, Soutis C, Potluri P. Bolted joints in three axially braided carbon fibre/epoxy textile composites with moulded-in and drilled fastener holes. Appl Compos Mater 2017;24:449–60. https://doi.org/10.1007/s10443-016-9542-z.
[13] Durão L, Tavares J, de Albuquerque V, Marques J, Andrade O. Drilling damage in composite material. Materials (Basel) 2014;7:3802–19. https://doi.org/10.3390/ma7053802.
[14] Tsao CC, Hocheng H. Effects of exit back-up on delamination in drilling composite materials using a saw drill and a core drill. Int J Mach Tools Manuf 2005;45:1261–70. https://doi.org/10.1016/j.ijmachtools.2005.01.015.
[15] Mattheij P, Gliesche K, Feltin D. Tailored fiber placement-mechanical properties and applications. J Reinf Plast Compos 1998;17:774–86. https://doi.org/10.1177/073168449801700901.
[16] Khaliulin VI, Khilov PA, Toroptsova DM. Prospects of applying the tailored fiber placement (TFP) technology for manufacture of composite aircraft parts. Russ Aerronautics 2015;58:495–500. https://doi.org/10.3103/S1068799815040236.
[17] Uhlig K, Spickenheuer A, Gliesche K, Karb I. Strength of CFRP open hole laminates made from NCF, TFP and braided preforms under cyclic tensile loading. Plast, Rubber Compos 2010;39:247–55. https://doi.org/10.1179/174328910X12647080902772.
[18] Gliesche K, Hübner T, Orawetz H. Application of the tailored fibre placement (TFP) process for a local reinforcement on an "open-hole" tension plate from carbon/epoxy laminates. Compos Sci Technol 2003;63:81–8. https://doi.org/10.1016/S0266-3538(02)00178-1.
[19] Koricho EG, Khomenko A, Fristedt T, Haq M. Innovative tailored fiber placement technique for enhanced damage resistance in notched composite laminate. Compos Struct 2015;120:378–85. https://doi.org/10.1016/j.compstruct.2014.10.016.
[20] Crothers PJ, Drechsler K, Feltin D, Herszberg I, Kruckenberg T. Tailored fibre placement to minimise stress concentrations. Compos Part A Appl Sci Manuf 1997;28:619–25. https://doi.org/10.1016/S1359-835X(97)00022-5.
[21] Grafil 34-700 by Mitsubishi Rayon Carbon Fiber & Composites 2010.
[22] Kravaev P, Stolyarov O, Seide G, Gries T. Influence of process parameters on filament distribution and blending quality in commingled yarns used for thermoplastic composites. J Thermoplast Compos Mater 2014;27:350–63. https://doi.org/10.1177/0892705712446167.
[23] Chiu SH, Liaw JJ. Fiber recognition of pet/rayon composite yarn cross-sections using voting techniques. Text Res J 2005;75:442–8. https://doi.org/10.1177/00405175054187.
[24] Kravaev P, Stolyarov O, Seide G, Gries T. A method for investigating blending quality of commingled yarns. Text Res J 2013;83:122–9. https://doi.org/10.1177/0040517512456760.
[25] ASTM-D3171-Standard Test Methods for Constituent Content of Composite Materials. ASTM Int 2010;15:1–6. doi:10.1520/D3529M-10.2.
[26] ASTM D 5229-92 – Standard Test Method for Moisture Absorption Properties and Equilibrium Conditioning of Polymer Matrix Composite Materials. Annu B ASTM Stand 2010;92:1–13. doi:10.1520/D5229.
[27] ASTM D3039/D3039M Standard test method for tensile properties of polymer matrix composite materials. Annu B ASTM Stand 2014:1–13. doi:10.1520/D3039.
[28] ASTM D5766 Standard Test Method for Open-Hole Tensile Strength of Polymer Matrix Composite. ASTM Stand 2013:1–7. doi:10.1520/D5766.
[29] Selver E, Potluri P, Hogg P, Soutis C. Impact damage tolerance of thermoset composites reinforced with hybrid commingled yarns. Compos Part B Eng 2016;91:522–38. https://doi.org/10.1016/j.compositesb.2015.12.035.
[30] Saleh MN, Yudhanto A, Potluri P, Lubineau G, Soutis C. Characterising the loading direction sensitivity of 3D woven composites: effect of z-binder architecture. Compos Part A Appl Sci Manuf 2016;90:577–88. https://doi.org/10.1016/j.compositesa.2016.08.028.
[31] Yang QQ, Gao CF, Chen WT. Stress concentration in a finite functionally graded material plate. Sci China Physics, Mech Astron 2012;55:1263–71. https://doi.org/10.1007/s11433-012-4774-x.
[32] Jones R. Mechanics of Composite Materials. Taylor & Francis; 1998.
[33] Callus PJ. The effects of hole-size and environment on the mechanical behaviour of a quasi-isotropic AS4/3501-6 laminate in tension, compression and bending. Air Veh Div Def Sci Technol Organ 2007:1–82.